Aust. Met. Mag. 34 (1986) 149-154 551.574.13

A case study of ice particle growth in a mixed-phase altostratus cloud

G.W. Paltridge, W.J. King and **C.M.R. Platt**
CSIRO Division of Atmospheric Research,
Aspendale, Australia

(Manuscript received November 1986; revised December 1986)

Detailed microphysical measurements in a mixed-phase altostratus cloud deck suggest that the diffusive growth rate of the ice particles is perhaps two or three times the theoretical expectation for spheroidal particles. A possible implication is that the average ventilation coefficient of the irregular falling ice crystals of the present case study (whose effective radii range from about 300 to 1200 μm) is about 4 or 5 – rather larger than that of spheroidal particles.

Introduction

This paper reports microphysical measurements obtained in a mixed-phase altostratus cloud during an extensive clouds-and-radiation experiment at Mildura, Australia, in June 1985. The measurements were collected using the CSIRO F-27 research aircraft whose instrumentation on that occasion is described elsewhere (Paltridge 1986). On June 18, two vertical profiles of an extensive and persistent As deck were obtained about 45 minutes apart. The aircraft followed the general easterly movement of the deck so that each profile (a slow descent at constant heading) was obtained in roughly the same patch of cloud. As a consequence it is possible to compare the observed growth of the particle size spectra with theoretical calculation.

The raw data relevant to the discussion are presented in Figs 1 to 4. From Fig. 1 in particular it is apparent that the simplest conception of the situation is to divide the cloud into two layers. The lower layer (2600 m to 3300 m altitude) was super-saturated with respect to both water and ice which implies an effective general upward velocity u_U. In the upper layer (3300 m to 3600 m altitude) the raw measurements indicate an apparently subsaturated atmosphere with mixing ratio r decreasing rapidly with height towards the cloud top at the base of the inversion. Bearing in mind that the raw measurements of r were of five-second averages, this apparent sub-saturation can be explained in terms of horizontal movement of the aircraft through some sort of cellular structure in the layer. Presumably this structure was associated with entrainment of dry air down through the inversion so that, on average, as the aircraft passed through several cells, the instrument recorded apparent sub-saturation. It is significant that the liquid water in this mixed-phase cloud was virtually confined to the upper layer (see Fig. 2). Again bearing in mind that the readings were averages over five seconds, this suggests sufficient velocity in the upward arms of the individual cells to create an oversupply of water substance in those arms – more, that is, than could be quickly converted to ice.

Fig. 1 Mixing ratio (r) for profile 2 (13.54 h to 14.09 h) and temperature (T_1) for profile 1 (13.03 h to 13.15 h) and temperature T_2 for profile 2. The dashed curves of r_i and t_w are the calculated saturation mixing ratios over ice and water respectively.

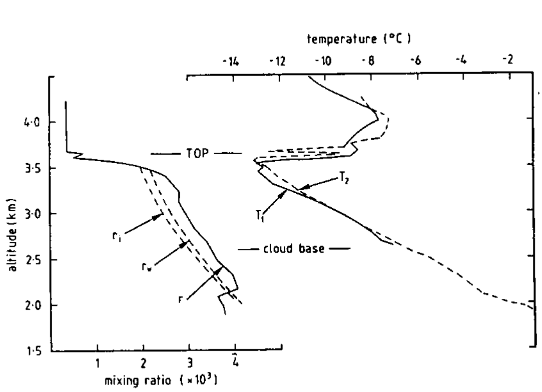

Fig. 2 Liquid water content for profile 1 (the open circles) and profile 2 (the solid dots). Note the 'wild' points at 3650m – see text. Measured with the CSIRO hot-wire instrument.

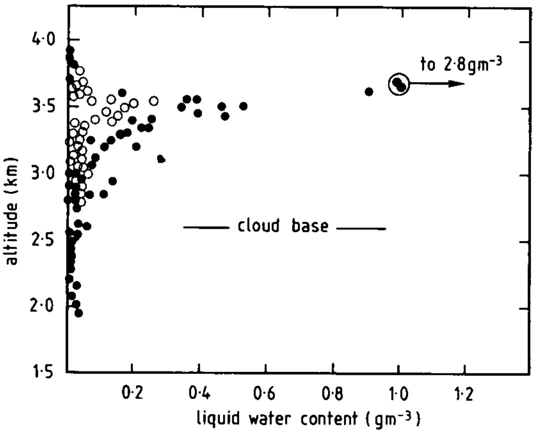

Fig. 3 Ice water content for profile 1 (the open circles) and profile 2 (the solid dots). These were calculated from the OAP Knollenberg probe on the basis of spherical particles.

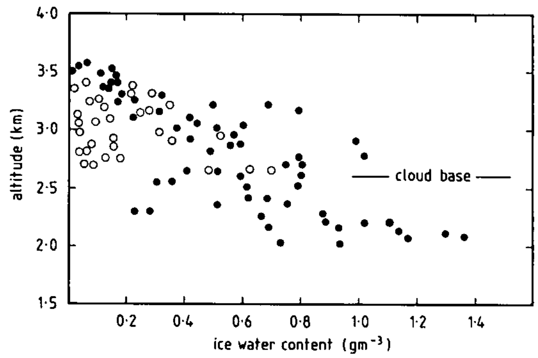

Fig. 4 Long wave fluxes measured by Eppley pyrradiometers. Solid dots from profile 2, open circles from profile 1.

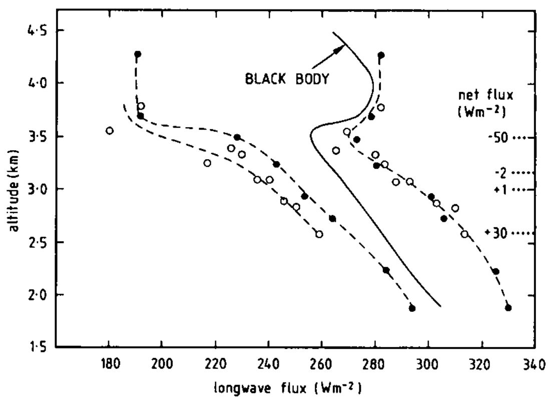

Figure 5 displays the two ice-particle size spectra obtained as averages over the times which the descending aircraft spent in each cloud layer during the first profile. The corresponding spectra from the second profile 45 minutes later are also shown. The rest of the paper addresses the question as to whether the change in lower layer particle size spectrum over the 45 minutes conforms to theoretical expectation.

Analysis and results

The relevant basic equation for the time rate of change of particle numbers of radius a is as follows:

$$\frac{dN_a}{dt} = \frac{\partial N_a}{\partial a} \cdot \frac{da}{dt} + \frac{\partial N_a}{\partial z} \cdot u(a) \qquad \ldots 1$$

where N_a is the number of ice particles of radius a, z is altitude, t is time and u(a) is the net vertical velocity of the particles. The first term on the RHS takes account of particle growth as a result of water vapour diffusion. The second term takes account of change in number density due to the difference in number of particles falling into the level and the number falling out. In the following, the theoretically derived factors da/dt and u(a) are discussed first and the experimentally determined factors $\partial N_a/\partial a$ and $\partial N_a/\partial z$; are discussed last.

Fig. 5 Measured particle size spectra from the OAP Knollenberg probe (for sizes > 300 μm) and from the 2-D Knollenberg spectrometer (for sizes < 400 μm).

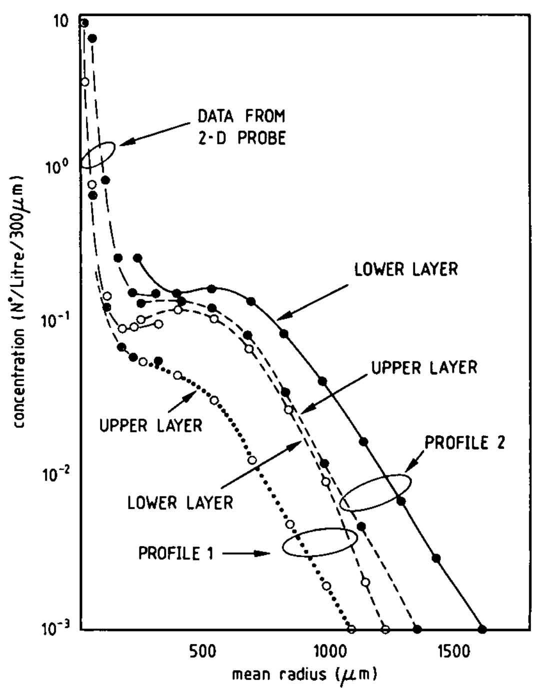

With regard to da/dt there is a fairly well-developed theory covering the diffusive growth of ice particles. According to Hall and Pruppacher (1976), Pruppacher and Klett (1978) or Stephens (1983) for instance, the governing equation for diffusion of water vapour to a particle is as follows where m_a refers to the mass of a single particle of radius a:

$$\frac{dm_a}{dt} = 4\pi C f D_v[\rho_v - \rho_v(T_s)] \qquad \ldots 2$$

Here C is the 'capacity' of the particle (= a for spheres); D_v is the water vapour diffusivity of air; p_v is the vapour concentration of the ambient air (the measured super-saturated value here – not the saturated value $\rho_v(T_\infty)$ at the temperature T_∞ of the ambient air); and $\rho_v(T_s)$ is the saturated vapour concentration over ice at the temperature T_s of the particle surface (see note attached to Table 1). The f is a ventilation coefficient which takes account of the fact that the particle is moving relative to its local atmosphere.

There is an equivalent equation governing the flow of heat from the particle. That is

$$L_s\frac{dm_a}{dt} = 4\pi C f k_A(T_s - T_\infty) \qquad \ldots 3$$

where on this occasion L_s is the latent heat of sublimation of ice and k_A is the thermal conductivity of air. This assumes a steady state whereby the release of latent heat from the diffusing water vapour is balanced by the heat conducted away. There should in principle be a further term on the RHS of Eqn 3 to take account of infrared radiative heat loss (or gain) by the particle. The point will be examined later in the paper, but at this stage it is simply necessary to say that, according to calculation from the infrared flux measurements of Fig. 4, the net radiative exchange of a particle at the mid-level of the lower layer is very small – less than 1 per cent of its sensible heat exchange.

Equations 2 and 3 can be solved simultaneously using a linear approximation for $\rho_v(T_s)$ given as a note attached to Table 1. This yields dm_a/dt as a function of known constants L_s, D_v, and k_A; of the measured T_∞, and of the 'unknowns' C and f. These last are unknown because they depend among many other things on particle shape. Referring to Table 1 for the various numerical values, and limiting oneself to the range of air temperatures from -15°C to -8°C, a good approximation to the solution is as follows:

$$\frac{dm_a}{dt} = 1.54\cdot 10^{-6} F_o a \text{ gm sec}^{-1} \qquad \ldots 4$$

where a is in cm and F_o is a single symbol representing the product of the unknowns f and 'normalised' capacity C/a. Assuming the particles to be spherical, this leads to

$$\frac{da}{dt} = 12.3\cdot 10^{-8} F_o/\rho\, a \text{ cm sec}^{-1} \qquad \ldots 5$$

where ρ is the density of the ice in the particles. In the later discussion, the symbol F represents F_o/ρ (i.e. $fC/a\rho$).

Referring now to the vertical velocity u(a) in Eqn 1, this is the net of the terminal velocity u_∞ of the particles and the general upward velocity u_U of the medium. (There must be an effective upward velocity of the medium in order to maintain the observed supersaturation.) From Kajikawa (1972) it is apparent that a linear approximation relating u_∞ to radius a is as good a generalisation as any in the absence of detailed information on particle shape. Thus we write

$$u(a) = Aa + u_U \qquad \ldots 6$$

where A is a constant of proportionality between u_∞ and a. The positive direction is downwards and u_U is therefore negative. In practice A depends enormously on particle shape and character, and therefore in the present context (even as an average) is an 'unknown' relevant only to the present cloud.

The factor $\partial N_a/\partial a$ in Eqn 1 is the slope of the particle size spectrum at radius a and at the specific time t. Similarly, the factor $\partial N_a/\partial z$ is the vertical gradient of concentration of particles of radius a at that time. In order to make use of the experimentally available data on these quantities, Eqn 1 can be recast in finite difference form as follows:

$$\frac{\Delta N_a}{\Delta t} \sim \left.\frac{\partial N_a}{\partial a}\right|_{t=o} \cdot \frac{da}{dt} + \left.\frac{\partial N_a}{\partial z}\right|_{t=o} \cdot u(a) \qquad \ldots 7$$

where the $\partial N_a/\partial a$ and $\partial N_a/\partial z$ are the slope and vertical gradient appropriate to the measurements in the lower layer at time t = 0 (i.e. to measurements during the first profile); and $\Delta N_a/\Delta t$ is the observed rate of change of number concentration in the lower layer (i.e. the number concentration change from the first to the second profile divided by the time between the profiles).

Table 1. Numerical values relevant to the present calculations for the lower layer whose average height was 2950 m.

c_p	Specific heat at constant pressure	0.24 cal g^{-1}K^{-1}
L_s	Latent heat of sublimation	676 cal g^{-1}
k_A	Conductivity of air	$5.6\cdot 10^{-5}$ cal cm^{-1} sec^{-1}K^{-1}
D_v	Diffusivity of water vapour in air	0.3 cm^2 sec^{-1}
r	Mixing ratio of water vapour	$3.1\cdot 10^{-3}$
T_∞	Ambient air temperature	264 K
T_s	Particle temp. (from solution Eqns 2 and 3)	265.6 K
g	Acceleration due to gravity	980 cm sec^{-2}
ρ_A	Density of air	$0.94\cdot 10^{-3}$ g cm^{-3}
ρ_v	Ambient vapour density	$3.0\cdot 10^{-6}$ g cm^{-3}
ρ	Density of ice particle	0.9 g cm^{-3}
Γ	Lapse rate	$7.0\cdot 10^{-5}$ K cm^{-1}

Note: The following linear approximation for the saturated vapour concentration over ice was used (it is accurate to within 5 per cent over the range −15°C to −8°C.

$$\rho_v(T_s) = 0.166\,(T_s\text{-}250)\cdot 10^{-6} \text{ g cm}^{-3}.$$

One can make use also of the pseudo-adiabatic thermodynamic equation to equate the supply of water substance due to the uplift of air at velocity u_U to the total mass growth rate of all the ice particles in unit volume. Thus

$$\left[\left(\frac{c_p}{L_s}+\frac{r}{T_\infty}\right)\Gamma-\frac{g}{L_s}\right]\rho_A u_U=\sum_{a=o}^{\infty}\frac{dm_a}{dt}\cdot N_a\cdot\Delta a \quad \ldots 8$$

The LHS is the rate of supply of water substance [derivable in this form from List (1968, p.323)], where c_p is the specific heat at constant pressure, Γ, is the lapse rate, g is the acceleration due to gravity and ρ_A is the density of air. The RHS via Eqn 4 is again a function of the unknown F. The equation relates the two unknowns u_U and F.

The solid curve of Fig. 6 is the observed $\Delta N_a/\Delta t$ over the particle size range 400-1200 μm radius. This is the range over which the OAP measuring device is reliable, and is the range which in any event contains the particles contributing to over 95 per cent of the total growth of ice. In principle therefore, one can apply Eqn 7 to two particle sizes (say, 500 μm and 1000 μm radius), and make use of Eqn 7., in order to obtain three equations containing the three unknowns F, u_U and A. Solution of these equations yields the following 'face' values:

$F \sim 5.5$
$u_U \sim 8 \text{cm sec}^{-1}$
$A \sim 160 \text{sec}^{-1}$

Now the factors $\partial N_a/\partial a$ and $\partial N_a/\partial z$ change with time as the size spectrum changes, so that an equally valid finite difference approximation of Eqn 1 involves replacing the initial profile values of $\partial N_a/\partial a$ and $\partial N_a/\partial z$ in Eqn 7 with the final profile values. When this is done, solution of the three equations as above yields a somewhat different set of 'face' values for the unknowns. That is

$F \sim 3.5$
$u_U \sim 10 \text{ cm sec}^{-1}$
$A \sim 100 \text{ sec}^{-1}$

Acceptable values should lie somewhere between the two extremes. In particular, the calculations suggest a value of F of the order of 4 or 5.

Discussion

The derived values of general upward velocity u_U and terminal velocities u_∞ (=Aa) are reasonable but uncheckable. Accepting all the assumptions inherent in the general argument, it appears that a u_U of about 8-10cm sec^{-1} is just balancing the terminal velocity of 700 μm particles. Smaller particles are rising and larger particles are falling. Referring to Fig. 3, there is in fact a considerable fall-out of large particles below the cloud base.

The significant point about the calculations is that the value of F is somewhat larger than the value one might expect based on theory and experiment with single and 'regular' ice particles.

Fig. 6 The solid curve is the concentration growth rate (simple subtraction of the dashed curves). The solid circles are calculated growth rates as per text.

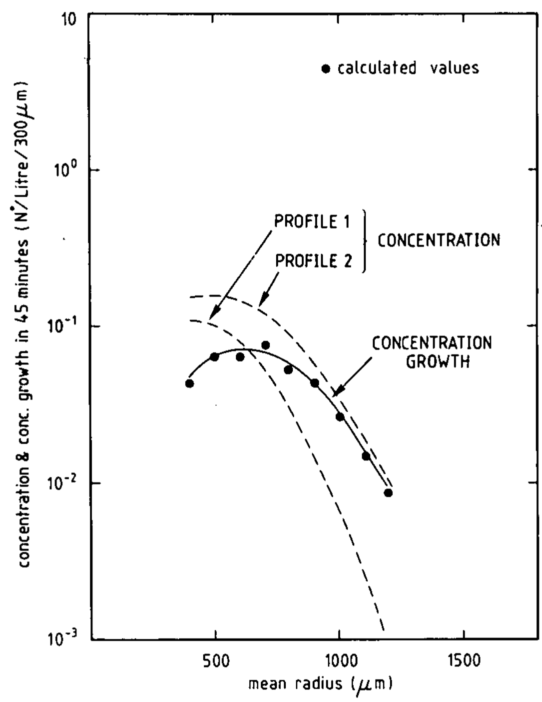

F (= Cf/aρ) involves various parameters which depend on particle shape and character. The capacity C can be calculated for regular shapes such as hexagonal plates or rhombic columns, etc., and is generally of the same order but somewhat less than a (see Pruppacher and Klett 1978, for instance). The density of ice particles is usually of the order of 0.9. The ventilation coefficient f is theoretically a function of Reynolds and Schmidt numbers (see again Pruppacher and Klett) and for the conditions here and for spheres and oblate spheroids should be about 1.2 for 500 μm radius particles and 1.6 for 1000 μm radius particles. So that, at least for spheres and oblate spheroids, one would expect F (which represents some average value appropriate for calculations over the entire size range) to be of this order – that is, something in the range of 1 to 2.

The ice particles in real clouds rarely have the simple shapes which can be handled mathematically. For what it is worth, the aircraft of the present experiment carried a 2-D Knollenberg spectrometer which gave information on the shapes of particles smaller than 300 μm. These shapes were simply 'irregular' – there was no evidence of the predominance of any specific type of particle.

Irregular particles have a high surface to volume ratio, so that in principle one might expect ventilation to be more significant for them than, say, for spheres and spheroids. It is at least qualitatively acceptable that, for the ensemble of irregular particles in the present cloud (and for similar ensembles of particles in other clouds), the average ventilation coefficient f is of the order of 4 or 5. 'Average' here refers to all the particles within the size range of the present calculations and measurement – that is, particles whose equivalent radius is roughly in the range 400 to 1100 μm.

As defined and discussed above, the factor F contains both the particle capacity C and the density ρ – neither of which is well defined for irregular particles. The result therefore should perhaps be more carefully stated. Namely, that on the assumption of values of C and ρ normally relevant to spheroidal particles, the experiment suggests a ventilation coefficient f for the present irregular particles of the order of 4 or 5. Put another way, it appears that the overall F (which one might call a 'growth correction factor' for irregular falling particles) is 2 or 3 times the expected value for spheroidal particles.

There are of course a number of factors which limit the reliability of the calculations.

There is an overriding assumption that the macroscopic cloud conditions were constant during the period of the measurement. The most that can be said is that the cloud was persistent and long-lived with no strong evidence of non-steady boundary conditions. There was some evidence of larger-scale cellular structure within the cloud (larger that is than the cells associated with entrainment in the upper layer – see for instance the 'wild' values of very large liquid water content at 3650 m which indicate passage of the aircraft through an individual cell which had rapidly brought air from the base to the top of the cloud). It has to be assumed for the purposes of this analysis that the several-minute averages of the particle size spectra have smoothed out any fluctuations associated with such structure.

It has been assumed also that radiative effects are insignificant. Referring back to the discussion of Eqns 2 and 3, radiative cooling of the particles would lower their temperature and hence increase the gradient of vapour pressure which governs diffusion to the ice surface. It was pointed out that the small net radiative exchange at the mid-level of the lower layer (see Fig. 4) is not significant. However it is conceivable that, if there was some cellular structure and motion within the lower layer, the average particle might move up and down within the layer and be exposed on occasion to higher rates of radiative exchange. One can perform a simple radiative flux calculation on the worst-case assumption of 100 per cent infrared absorption (or emission) efficiency for particles at the very top and the very bottom of the cloud. For 1000 μm radius particles, their radiative loss at the top or their radiative gain at the bottom would be less than 10 per cent of their conductive heat loss. It is difficult to imagine any form of cellular motion which would produce an average radiative exchange more than a few per cent of the conductive heat loss for particles whose average position is at the mid-level of the lower layer.

The possibility of a significant contribution to particle growth by coalescence can almost certainly be discounted. By a collision frequency argument, and by assuming an unlikely 100 per cent efficiency of collection by a particle falling through the field of all particles smaller than itself, it is possible to calculate the maximum growth rate of a particle of radius a due to coalescence according to

$$\left.\frac{dm_a}{dt}\right|_c = \frac{4\pi^2 \rho A a^2}{3} \sum_{x=o}^{a-\Delta x} N_x (a-x) x^3 \Delta x \qquad \ldots 9$$

where the summation is over all particles of radius x less than a in steps of Δx, and the subscript c refers only to the coalescence process. Using values of N_x from the present experiment, the maximum value of dm_a/dt_c for the largest particles (say 1000 μm) is at least 50 times smaller than the corresponding diffusive growth rate dm_a/dt.

The most doubtful input data to the calculations is of the vertical gradient $\partial N_a/\partial z$. Its value depends on an assumption of a constant vertical gradient through the cloud. Further, it relies on the measurement of N_a in the upper layer where there was apparently cellular motion and entrainment. There can be some argument about whether the average N_a measured in such circumstances is the correct quantity to use for calculation of $\partial N_a/\partial z$. However the sensitivity of F to error in $\partial N_a/\partial z$ is not large. A fifty per cent change in $\partial N_a/\partial z$ applied to both radii used in the calculation leads to a change in the derived value of F of only 0.5. The sensitivity to N_a of the upper layer is almost an order of magnitude less.

The solid points of Fig. 6 are the calculated growth rates for each 100 μm increment in radius over the range 400 to 1200 μm. They don't add too much to the argument since the 500 and 1000 μm radius observed values have been used to derive the values of F, u_U and A which were used in the calculations. (Note that the application of Eqn 7 to generate the points was with the initial profile values of $\partial N_a/\partial a$ and $\partial N_a/\partial z$ and the corresponding values of F, u_U and A.) The question arises as to the sensitivity of the calculated F to the choice of the pair of radii. Adjacent pairs (i.e. pairs only 100 μm apart) can give outrageous values. However, by pairing one radius from 500, 600 and 700 μm with another radius from 900, 1000 and 1100 μm, nine values of F can be derived which range from 4.3 to 6.4. This is a significant range, but is not large enough to negate the basic result – namely, that the 'observed' value of F (and most probably of the actual ventilation coefficient f) is probably about 2 or 3 times the value to be expected for regular (i.e. spheroidal) particles.

References

Hall, W.D. and Pruppracher, H.R. 1976. The survival of ice particles falling from cirrus clouds in sub-saturated air. *J. Atmos. Sci., 33*, 1995-2006.

Kajikawa, M. 1972. Measurements of falling velocity of individual snow crystals. *J. met. Soc. Japan, 50*, 577-84.

List, R.J. 1968. *Smithsonian Meteorological Tables, Sixth Revised Ed.* Smithsonian Institution Press, Washington D.C., 527 pp.

Paltridge, G.W. 1986. Spectral and total albedo to solar radiation of ice and water clouds. Submitted to *J. Atmos. Sci.*, 1986.

Pruppracher, H.R. and Klett, J.D. 1978. *Microphysics of Clouds and Precipitation.* D. Reidel Publ. Co., Dordrecht, Boston, London, 714 pp.

Stephens, G.L. 1983. The influence of radiative transfer on the mass and heat budgets of ice crystals falling in the atmosphere. *J. Atmos. Sci., 40*, 1729-39.